

# Stock assessment of albacore tuna in the Indian Ocean using Bayesian State-Space Surplus Production Model

Sung Il Lee<sup>1</sup>, Toshihide Kitakado<sup>2</sup> and Doo Nam Kim<sup>1</sup>

<sup>1</sup>National Institute of Fisheries Science

<sup>2</sup>Tokyo University of Marine Science & Technology

## Abstract

A Bayesian state-space production model with the Pella and Tomlinson function was developed to assess the stock status of albacore tuna (*Thunnus alalunga*) in the Indian Ocean. The catch data used span from 1950 to 2017, and the joint standardized CPUEs of longline fleets were used as the abundance indices. As a result, for the base case which used CPUE of R34 with the initial year of 1950 and no increase in catchability, the median estimates of carrying capacity (K), maximum sustainable yield (MSY),  $B_{MSY}$ , and  $F_{MSY}$  were 290,003 ton, 93,933 ton, 128,890 ton and 0.748/year, respectively. And the ratios of  $B_{2017}/B_{MSY}$ , and  $F_{2017}/F_{MSY}$  for the base case were respectively estimated as 1.589, and 0.259, which indicate that the stock is not overfished and not subject to overfishing. However, in sensitivity analyses, the scenarios using CPUE of R3 showed that the stock is overfished and not subject to overfishing.

## Introduction

As age-aggregated population dynamics models, a state-space production model has been used. A merit of this model is a possible incorporation of random errors in both the population dynamics (i.e. process errors) and the observations (i.e. observation errors) (Meyer and Millar, 1999a). In this study, a stock assessment for the Indian Ocean albacore tuna was conducted by using a Bayesian state-space approach with Pella and Tomlinson function.

## Data and Methods

## 1. Data

The IOTC database (as of December, 2018) was used for the nominal catch of albacore tuna in the Indian Ocean (Fig. 1). The abundance indices used this study were the joint standardized CPUEs over main longline fleets (Japan, Korea and Taiwan) with vessel effects from 1979 to 2017 (Hoyle et al., 2019). We selected the joint indices for R34 and R3 because of the main area of longline fisheries fishing for albacore tuna. And as discussed at last IOTC WPTmT meeting (IOTC, 2019), the catchability ( $q$ ) assumed to be 1% increase per year for sensitivity analysis.

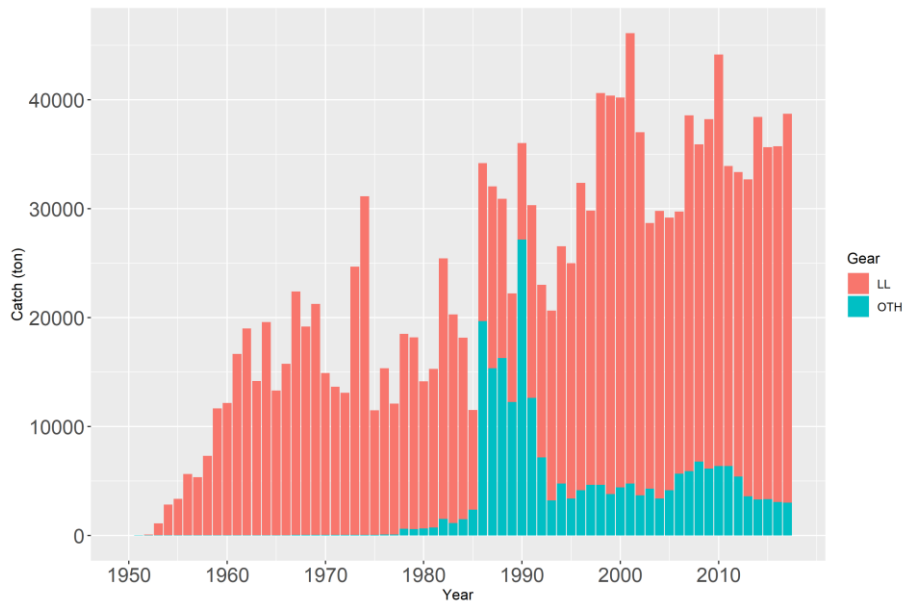


Fig. 1. Annual catch of albacore tuna by fleet (gear type) in the Indian Ocean, 1950-2017 (data source: IOTC database).

## 2. Bayesian state-space production model

A general deterministic model is expressed as

$$B_{t+1} = B_t + g(B_t) - C_t, \quad (1)$$

where  $B_t$ ,  $C_t$ , and  $g(B_t)$  are the biomass at the beginning of year  $t$ , the total catch during year  $t$ , and the surplus production function, respectively. In this study, we used Pella and Tomlinson form (Pella and Tomlinson, 1969) as the surplus production function:

$$g(B) = rB \left(1 - \left(\frac{B}{K}\right)^z\right), \quad (2)$$

where  $r$ ,  $K$ , and  $z$  are the intrinsic growth rate, the carrying capacity and the shape parameter, respectively.

The observed data are the annual catch ( $C$ ) and CPUE ( $I$ ), and the relative abundance index (CPUE) is expressed as biomass ( $B$ ) and catchability coefficient ( $q$ ).

$$I_t = qB_t \quad (3)$$

We can reparametrize equations (1) and (3) by expressing the annual biomass as a proportion of carrying capacity (Depletion level,  $D = B/K$ ) (Meyer and Millar, 1999b; Otsuyama and Kitakado, 2016), and assume process error and observation error of lognormal distribution as Bayesian state-space model.

$$D_{t+1} = \left(D_t + g(D_t) - \frac{C_t}{K}\right) e^{u_t}, \quad u_t \sim N(0, \tau^2) \quad (4)$$

$$I_t = qKP_t e^{v_t}, \quad v_t \sim N(0, \sigma^2) \quad (5)$$

where  $u_t$  and  $v_t$  are the process error and observation error in year  $t$ , respectively.

### 3. MCMC sampling

A MCMC method (Gibbs sampling) was used to estimate parameters of models and posterior distributions of parameters ( $r$ ,  $K$ ,  $D$ ,  $q$ ,  $\tau$ ,  $\sigma$ ). As there were non-informative prior distributions, a uniform distribution was used for all the parameters in the model. The range of prior distribution was set by the trial and error process. Checking the result of posterior distribution of each parameter, we adjusted the range of prior distribution to slightly wider than posterior distribution. As estimated values of each parameter, we employed posterior medians.

### 4. Model runs

As for the initial year of assessment, two years were considered that were 1950, the first year in which catch was recorded, and 1979 when botch catch and CPUE were available. We selected the scenario using CPUE of R34 with the initial year of 1950 and no increase in catchability as a base case, and the scenario using CPUE of R34 with initial year of 1950 and

an increase in catchability (scenario 1), the scenario using CPUE of R34 with initial year of 1979 and an increase in catchability (scenario 2), the scenario using CPUE of R3 with initial year of 1950 and no increase in catchability (scenario 3), and the scenario using CPUE of R3 with initial year of 1950 and an increase in catchability (scenario 4) as for sensitivity analyses. Therefore, a total of 5 scenarios were examined in this study.

## Result and Discussion

We iterated 3,000,000 simulations with 3 chains using a burn-in of 500,000 and a thinning of 500.

Trace plots and posterior densities for the model parameters of each scenario are shown in Fig. 2, and the statistics are summarized in Table 1. As can be seen in Fig. 2, the posterior distributions of carrying capacity ( $K$ ), catchability coefficient ( $q$ ), and observations error ( $\sigma$ ) are positively skewed. The median of carrying capacity ( $K$ ) and maximum sustainable yield (MSY) are estimated as 290,003 ton and 93,933 ton, respectively (see Table 1). However, the uncertainty is high in both parameter estimates due to the wide range of 95% credibility intervals.

Fig. 3 shows the convergence diagnostics of the model parameters, indicating that the factors of all parameters approached value of 1 and converged fully, along with the trace plots.

The difference between the estimated and the observed CPUEs is minor, and the predictive 95% credibility intervals cover all the observed CPUEs (Fig. 4). In terms of biomass estimates (Fig. 5), it sharply decreased at the beginning, 1951, and then there was no significant change over time other than showing a decline around 1989. The change of biomass is similar to the CPUE trend, which seems to be greatly affected by the CPUE. Furthermore, the range of 95% credibility intervals is wide as well.

The  $B/B_{MSY}$  ratio decreased dramatically at the beginning, and then showed a small decrease at a stable level (Fig. 6). In terms of the  $F/F_{MSY}$  ratio, although it is at low level but has gradually increased with a relatively high upper boundary of 95% credibility intervals (Fig. 7).

Fig. 8 shows the Kobe plots showing the trace of the stock status of Indian Ocean albacore tuna. For the base case, it indicates that the stock is not overfished and not subject to overfishing. However, in the case of scenarios 3 and 4 showed the stock is overfished and not subject to overfishing, and scenario 4 was a more pessimistic.



Table 1. Posterior medians of parameters for the Bayesian state-space surplus production model of each scenario

Scenario	$K$	$r$	$MSY$	$B_{MSY}$	$F_{MSY}$	$B_{2017}/B_{MSY}$	$F_{2017}/F_{MSY}$
base case	290,003	1.122	93,933	128,890	0.748	1.589	0.259
scenario1	327,521	0.722	69,598	145,565	0.481	1.042	0.533
scenario 2	347,523	1.084	118,918	144,935	0.834	1.179	0.277
scenario 3	260,348	0.945	72,181	115,710	0.630	0.997	0.534
scenario 4	391,176	0.553	63,562	173,856	0.369	0.662	0.917

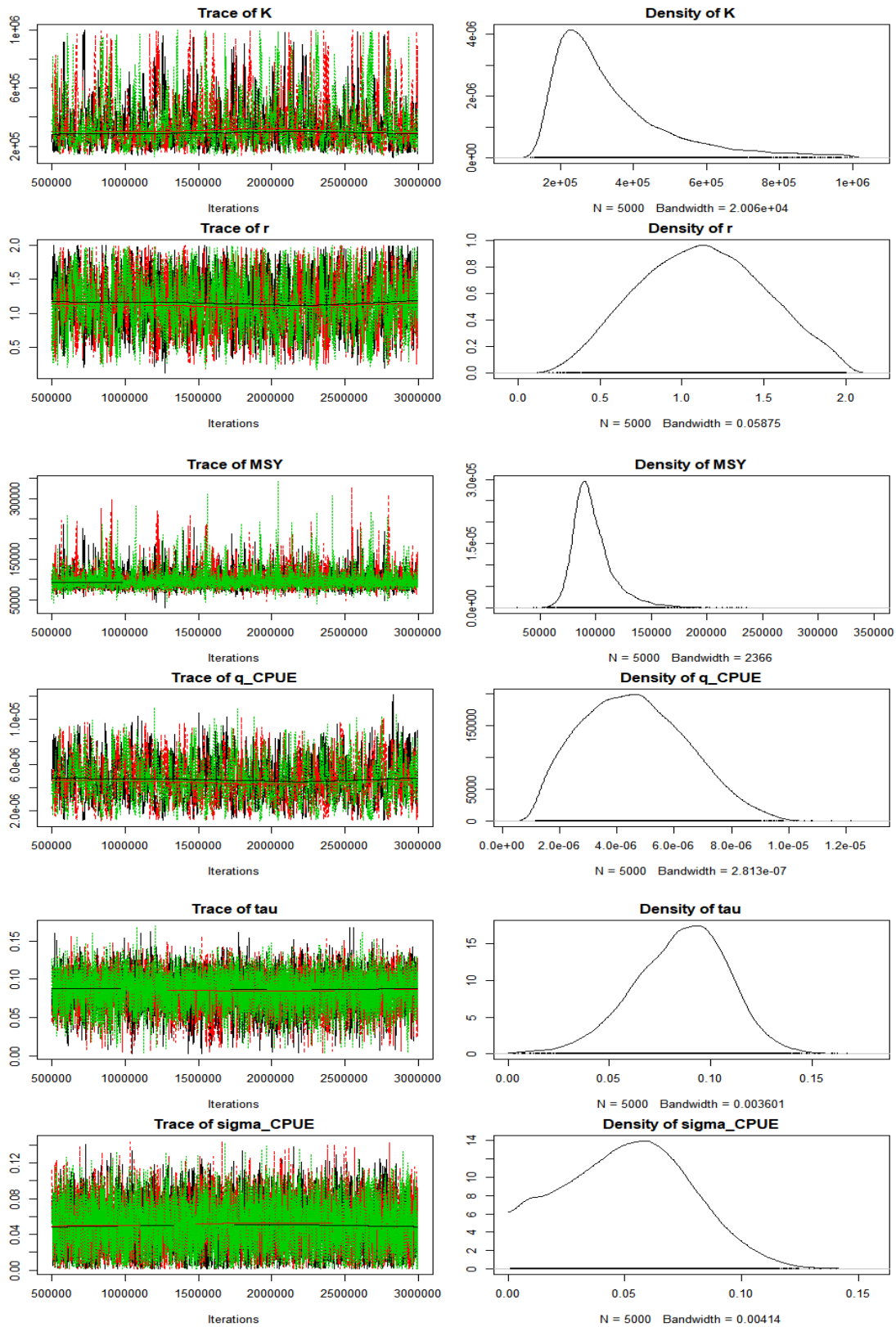


Fig. 2. Trace plots of the MCMC simulations and posterior distributions for the Bayesian state-space surplus production model parameters of the base case.

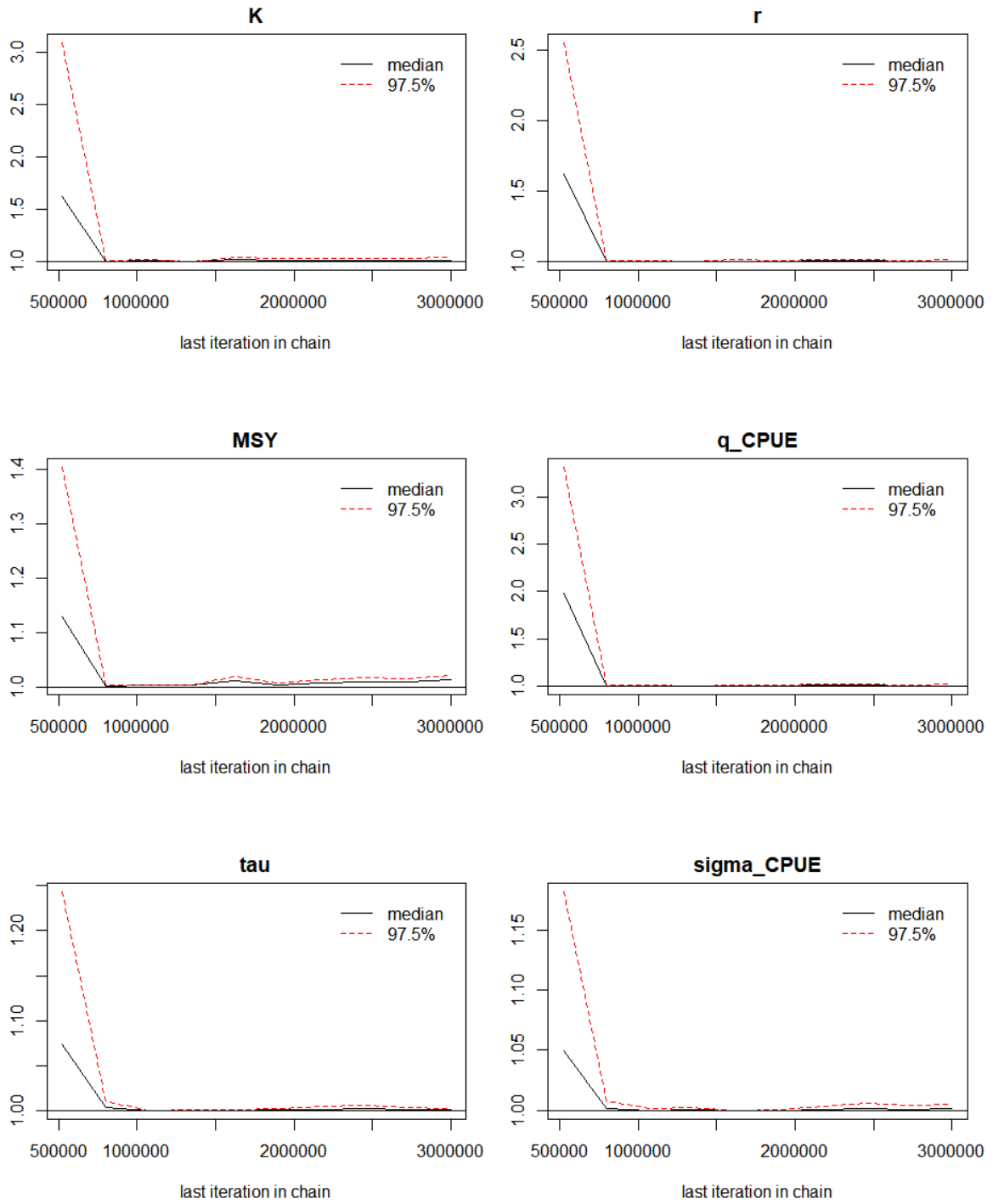
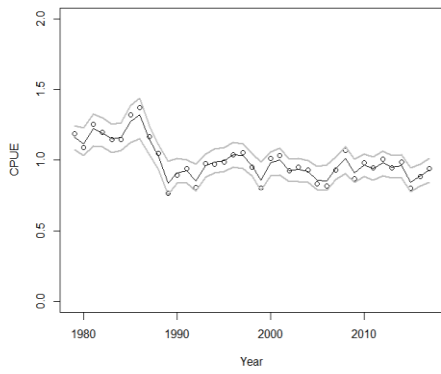
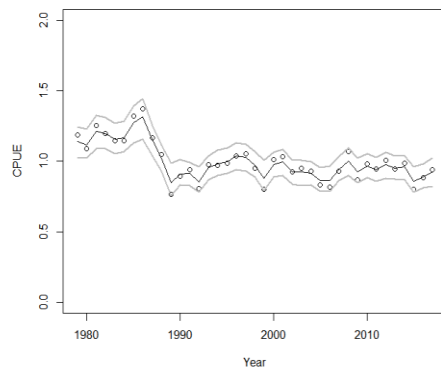


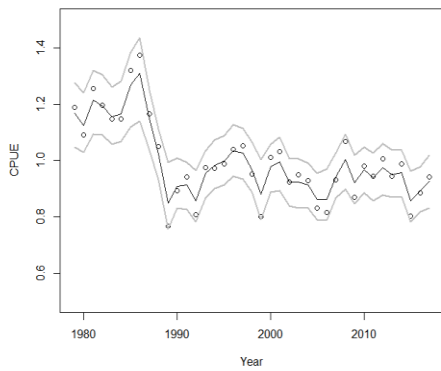
Fig. 3. Gelman plot diagnostics for assessing convergence of MCMC Chains for the Bayesian state-space surplus production model parameters of the base case.



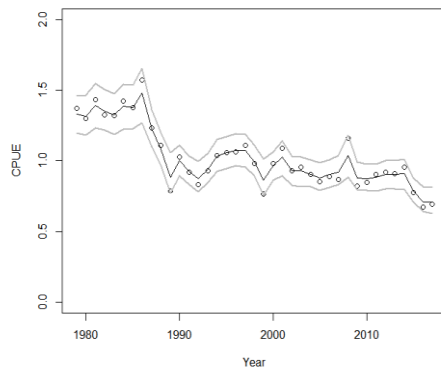
(a) base case



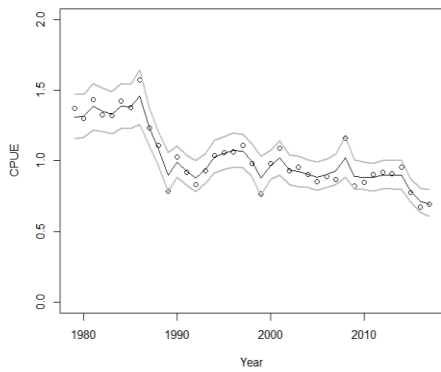
(b) scenario 1



(c) scenario 2



(d) scenario 3



(e) scenario 4

Fig. 4. Observed CPUEs and posterior means of the predicted CPUEs with 95% credibility interval by the Bayesian state-space surplus production model of each scenario.

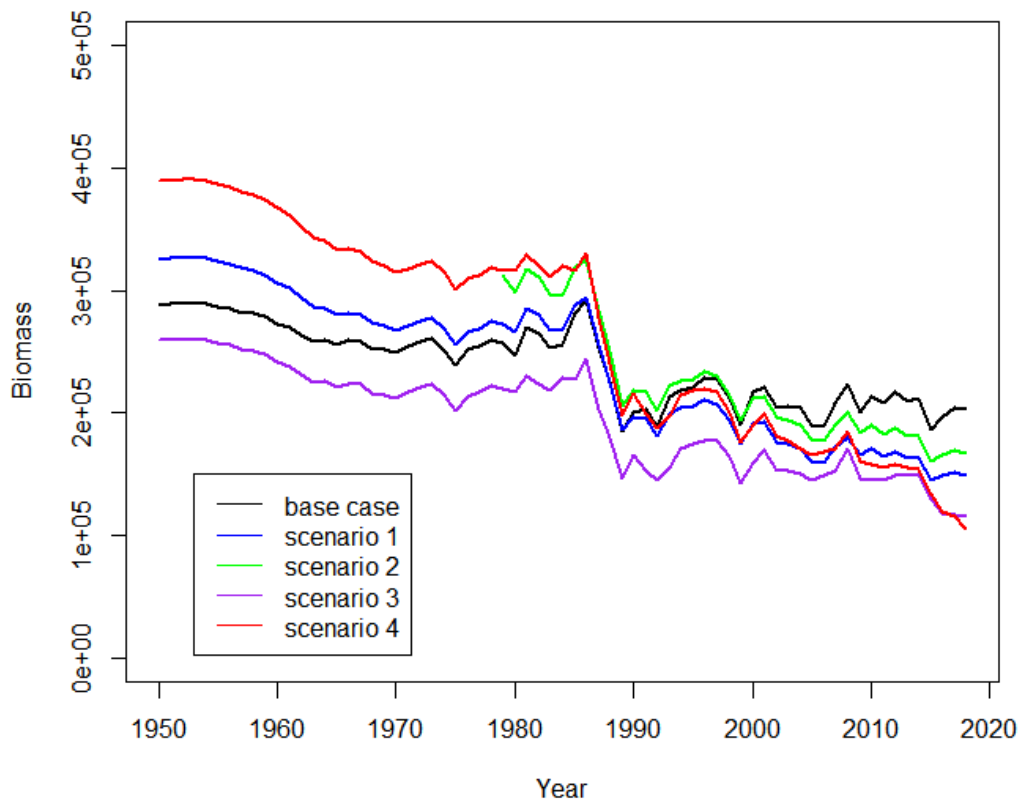


Fig. 5. Changes in biomass estimates by the Bayesian state-space surplus production model of each scenario.

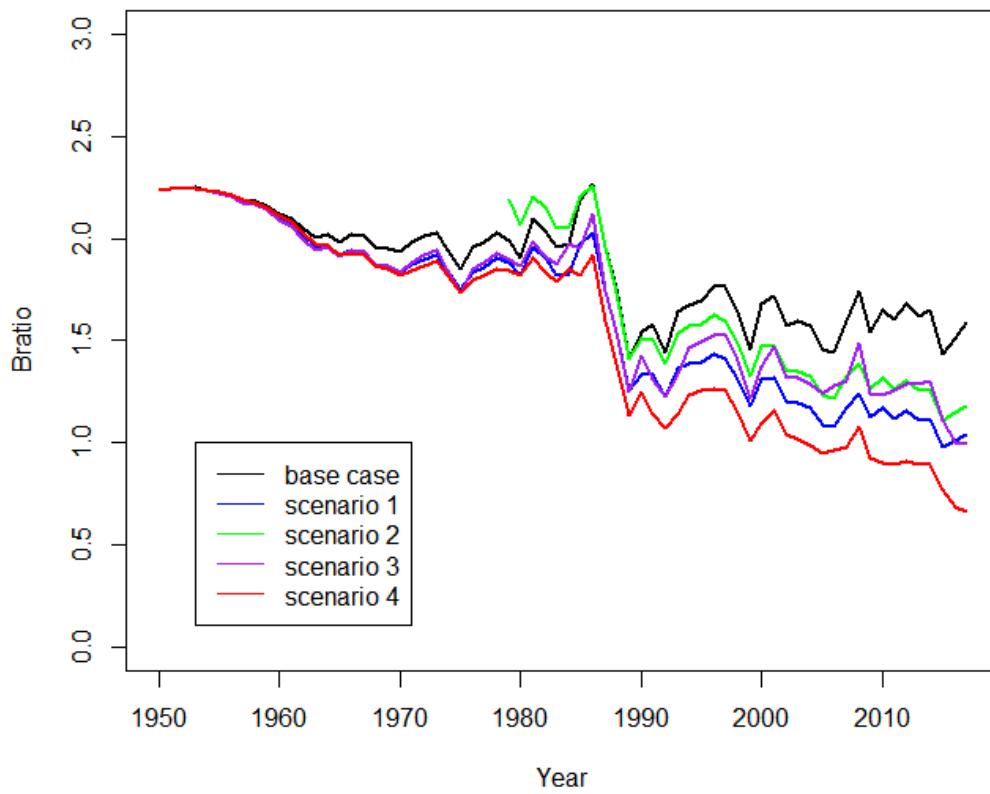


Fig. 6. Changes in  $B/B_{MSY}$  ratio by the Bayesian state-space surplus production model of each scenario.

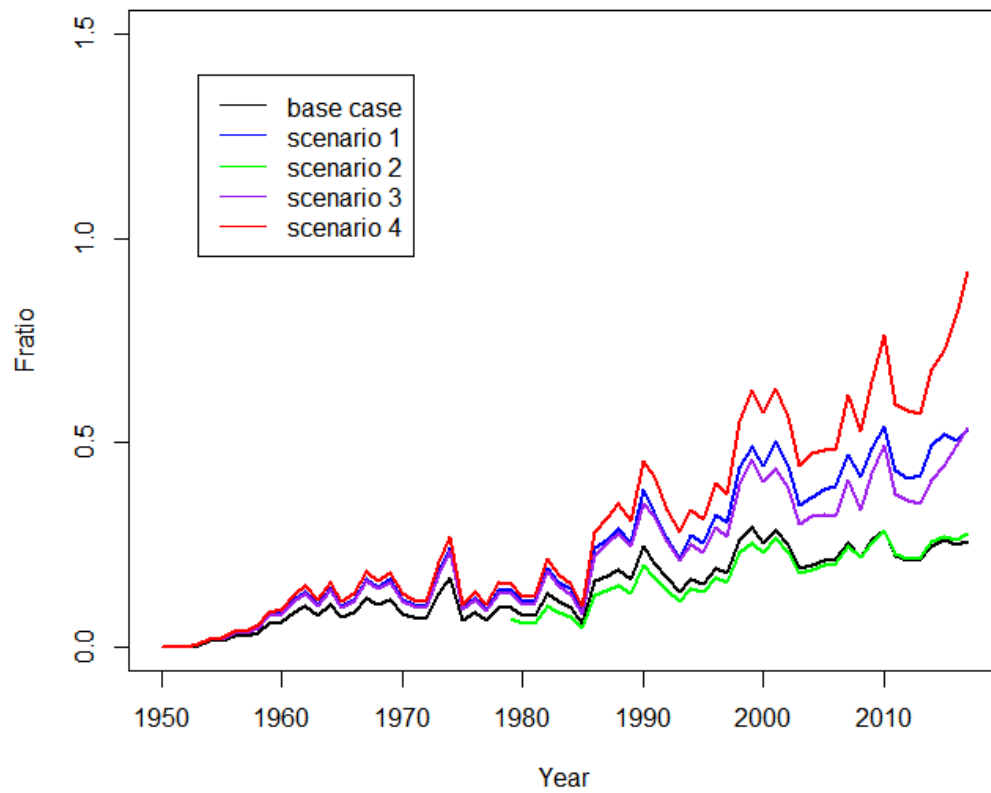
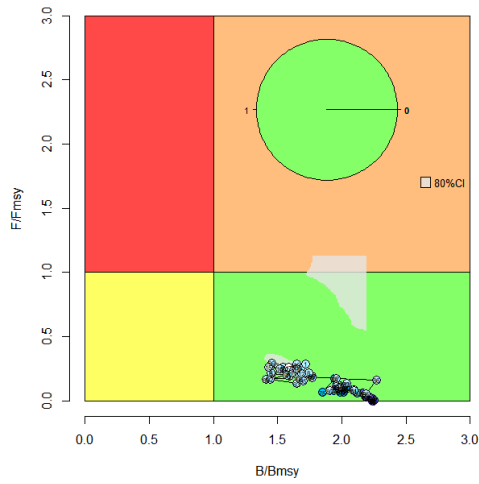
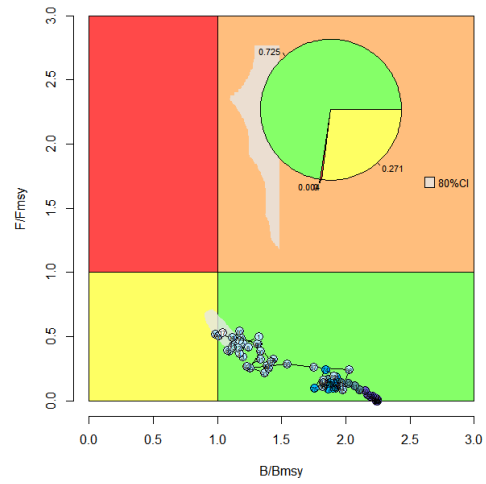


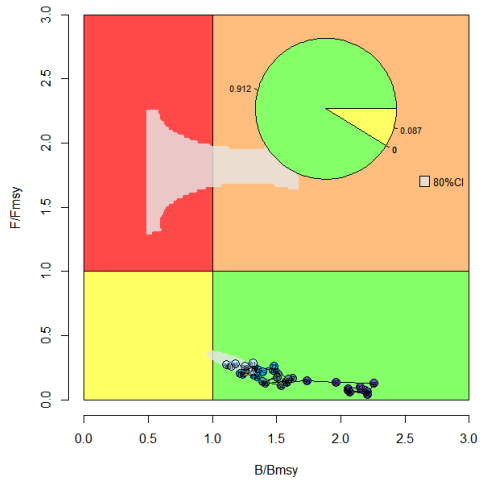
Fig. 7. Changes in  $F/F_{MSY}$  ratio by the Bayesian state-space surplus production model of each scenario.



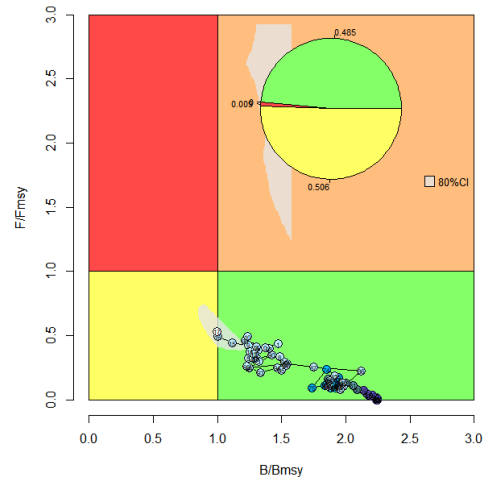
(a) base case



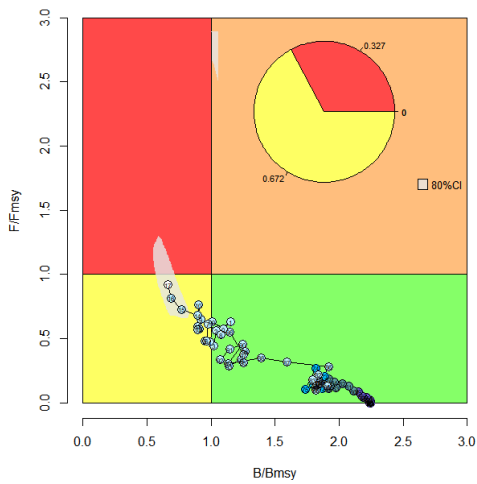
(b) scenario 1



(c) scenario 2



(d) scenario 3



(e) scenario 4

Fig. 8. Kobe plot for Indian Ocean albacore tuna by the Bayesian state-space surplus production model of each scenario.

## References

- Hoyle, D. S., D. Fu, D. N. Kim, S. I. Lee, T. Matsumoto, K. Satoh, S. P. Wang, and T. Kitakado. 2019. Collaborative study of albacore tuna CPUE from multiple Indian Ocean longline fleets in 2019. IOTC-2019-WPTmT(AS)-10.
- Indian Ocean Tuna Commission (IOTC). 2019. Report of the Seventh Session of the IOTC Working Party on Temperate Tunas (Data Preparatory Session). IOTC-2019-WPTmT(DP)-R[E].
- Meyer, R. and R. B. Millar. 1999a. Bayesian stock assessment using a state-space implementation of the delay difference model. *Can. J. Fish. Aquat. Sci.* 56: 37-52.
- Meyer, R. and R. B. Millar. 1999b. BUGS in Bayesian stock assessments. *Can. J. Fish. Aquat. Sci.* 56: 1078-1086.
- Otsuyama, K. and T. Kitakado. 2016. Bayesian state-space production models for the Indian Ocean bigeye tuna (*Thunnus Obesus*) and their predictive evaluation. IOTC-2016-WPTT18-19.
- Pella, J. J. and P. K. Tomlinson. 1969. A generalized stock production model. *Inter-American Tropical Tuna Commission*, 13, 419-496.